Rare Metal Materials and Engineering
Volume 48, Issue 7, July 2019
Available online at www.rmme.ac.cn

Science Press

Cite this article as: Rare Metal Materials and Engineering, 2019, 48(7): 2074-2083.

ARTICLE

Temperature Field of Temperature Controlled Roll for Magnesium Alloy

Li Yang[1], Ma Lifeng[1], Jiang Zhengyi[2], Huang Zhiquan[1], Lin Jinbao[1], Ji Yafeng[1]

[1] Heavy Machinery Engineering Research Center of the Ministry of Education, Taiyuan University of Science and Technology, Taiyuan 030024, China; [2] University of Wollongong, Wollongong NSW 2522, Australia

Abstract: Magnesium alloy sheet rolling has special control requirements on the temperature of the work rolls, so in this paper, the temperature of the rolls was controlled by fluid-solid coupled heat transfer. Based on the finite difference method, a differential model for the heat transfer process of roll and thermal oil was established, which was complemented by the corresponding experimental verification. A fluid-solid coupling heat transfer model was also established by FLUENT, which gives the roll temperature rise curve and the distribution of surface and cross-section temperatures during the heat transfer process. The results show that the temperature near the operating side of the roll is the highest, the temperature decreases gradually from the operating side to the driving side, and the temperature difference range between the operating side and the driving side is 5~12 °C, which is almost unaffected by the fluid temperature and speed. The maximum temperature difference between the inner wall and the outer wall of the roll is 6 °C, so it can be considered that the radial temperature distribution is even. Under different fluid temperatures and velocities, the temperature of the roll rises at a decreasing rate, and when the fluid temperature rises and the velocity increases, the temperature rise of the roll becomes faster. After the heating for the roll is stopped, its surface temperature does not immediately begin to drop and remains for a period of time, about 5~8 min, and the temperature and speed of the fluid have a small effect on the extended time. The calculated values of the average roll surface temperature agree well with the experimental values, and the maximum relative error is 8.3%, demonstrating that the finite differential model is effective, and can be used as part of the magnesium alloy plate rolling model.

Key words: magnesium alloy; finite difference method; coupled heat transfer model; temperature rise curve; temperature distribution; isothermal rolling

Magnesium alloy has significant advantages, such as small density, high specific strength, good heat dissipation, good shock resistance, good electromagnetic shielding performance and easy recycling [1-4]. It is widely used in aviation, aerospace, automobiles, high-velocity rail and electronics, and becomes the most promising non-ferrous metal materials [5]. The production methods of magnesium alloys mainly include casting, extrusion, forging and rolling, and among them, rolling is the most economical and effective way for producing magnesium alloy sheet. In the rolling process of magnesium alloy sheet, the contact between the roll and the sheet causes a large temperature drop of the sheet, resulting in deterioration of the plasticity of the magnesium alloy and defects such as edge cracks and surface cracks in the sheet of the magnesium alloy. During the rolling process, the roll temperature will gradually increase. When the roll temperature is too high, defects such as sticking of magnesium alloy sheet will be easily caused [6,7]. In addition, uneven temperature distribution on the roll surface will cause irregularities on the surface of the magnesium sheet, seriously affecting the yield of magnesium alloy sheet.

In the entire heating process for roller, the uniformity of the temperature distribution in the roller surface area and the uni-

Received date: July 20, 2018
Foundation item: National Natural Science Foundation of China (U1610253, 51604181); Key Research and Development Program of Shanxi Province (201603D111004, 201603D121010); Natural Science Foundation of Shanxi Province of China (201601D011012)
Corresponding author: Ma Lifeng, Ph. D., Professor, Heavy Machinery Engineering Research Center of the Ministry of Education, Taiyuan University of Science and Technology, Taiyuan 030024, P. R. China, Tel: 0086-351-2776769, E-mail: malifengtyust@163.com

formity of the roller circumference are mainly concerned. Rollers are usually heated by induction heating, flame heating, and resistance heating. Flame heating has disadvantages such as low heating efficiency, local high temperature on the roll surface, and difficulty in controlling the temperature distribution. Zhang Tingting [8] compared the induction heating method and the resistance heating method of the heating of the warm rolling mill roll, and found that when the temperature of the rolling section is set to the target temperature ±5 °C, the effective rolling section accounts for 50%, 33% of the entire roll width (uneven axial temperature distribution of roll). Li Tingting [9] simulated the temperature distribution of induction heating in warm rolling, setting the process temperature difference within 10 °C, and the effective rolling interval accounted for about 68% of the total length of the roll. The effective rolling interval can be increased to 81.6% and 83.2% by adjusting the air flow on the roll surface and the distribution of the magnetism (uneven axial temperature distribution of roll). Based on the above problems, a new type of roll heating method was proposed in this paper, a roll that is heated by the heat transfer between the thermal oil and the roll. It can solve the defects of low roll surface temperature and non-uniformity causing wrinkles on the sheet, and can solve the sticking roll defects caused by the high roll surface temperature due to plastic deformation heat by cooling using low-temperature oil, and can also solve problems such as small effective rolling zone of the roll (the more uniform the axial temperature distribution, the larger the effective rolling section) and difficulty in line heating. Therefore, it is possible to achieve online uniform temperature regulation of the rolls.

Based on the finite element method [10-13] and the basic laws of heat transfer theory, the finite difference equation of thermal oil heated rolls was established, which facilitates the rapid and real-time calculation for the instantaneous average temperature of the roll surface. The fluid-solid coupling model of thermal oil heated rolls was established by numerical simulation, which facilitates the heating process of the roller surface and the exploration of temperature distribution, and was supplemented by corresponding experimental verification. The calculated values of the roll surface average temperature field agree well with the experimental values, which verifies the correctness and validity of the finite difference model. The results of the study provide guidance for roll temperature control in the rolling process, which can solve the defects such as large convexity of the magnesium plate, severe wave shape, and sticking roll caused by the ineffective control of the roll temperature, and improve the rolling process of the magnesium alloy sheet. It is of great significance to increase the yield of rolled steel.

1 Experiment

Fig.1 shows the diagram of fluid heating roll. The experimental set-up in which roll was heated by thermal oil is shown in Fig.2. The oil temperature controller and the oil hose tubing with insulation cotton outside are connected into the loop. The roll is made of 9Cr2Mo and the model of thermal oil is L-QD330.

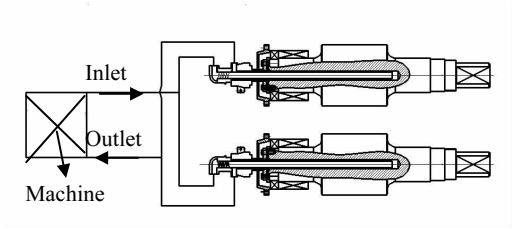

Fig.1 Diagram of fluid heating roll

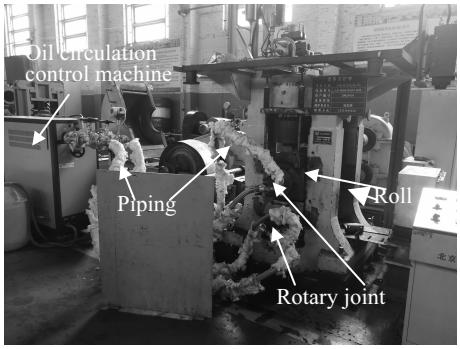

Fig.2 Diagram of experimental device

At different temperatures of 125, 150, 175 and 200 °C and at different flow velocities of 0.31, 0.46, 0.61 and 0.76 m/s, the temperature and speeds were randomly combined to generate 16 groups of experimental conditions. When the roll surface temperature reached an approximately equilibrium state, the heating was stopped and cooling naturally at ambient temperature.

8 points were averagely selected on the roll surface and the spacing of each point was 50 mm, recorded as T_1, T_2, T_3, T_4, T_5, T_6, T_7 and T_8. The average temperature T is the arithmetic average of T_1 to T_8. The temperature of the corresponding position was measured and recorded with thermocouple, as shown in Fig.3.

2 Governing Equations

2.1 Hypothetical conditions

1) The model of fluid heat transfer roll is simplified as one dimensional unsteady heat conduction model of a hollow cyl-

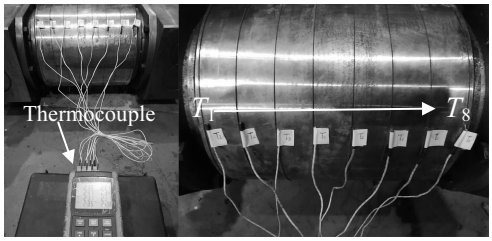

Fig.3 Diagram of actual measurement and record

inder, which is the heat transfer along the radial direction.

2) The physical property parameters of the roll and the fluid are not changed with time.

3) Boundary conditions for heat transfer between thermal oil and inner wall of the roll and the boundary conditions between the outer wall of the roll and the air are considered as the third kind of thermal boundary conditions.

2.2 Differential equations

The one-dimensional equation for transient heat conduction in a cylinder coordinate system is expressed as follows[14]:

$$\frac{\partial^2 T(r,t)}{\partial r^2}+\frac{1}{r}\frac{\partial T(r,t)}{\partial r}=\frac{1}{a}\frac{\partial T(r,t)}{\partial t},\ r_1<r<r_2,\ t>0 \tag{1}$$

where T is the temperature, r is the radius of hollow cylinder, t is time, and a is the thermal diffusivity.

The boundary and initial conditions are [14]:

$$T(r,0)=T(r) \tag{2}$$

$$-\lambda\frac{\partial T(r,t)}{\partial r}+h_1T(r,t)=f_1, r=r_1 \tag{3}$$

$$\lambda\frac{\partial T(r,t)}{\partial r}+h_2T(r,t)=f_2, r=r_2 \tag{4}$$

where λ is the thermal conductivity, h_1 is the convective heat transfer coefficient between the inner wall of the roll and thermal oil, h_2 is the convective heat transfer coefficient between the outer wall of the roll and air.

f_1, f_2 are expressed as:

$$f_1=h_1t_{f1} \tag{5}$$

$$f_2=h_2t_{f2} \tag{6}$$

where t_{f1} is the temperature of thermal oil and t_{f2} is the temperature of air.

2.3 Finite differential equations

The region is discretized into a grid with a step size of Δr and Δt, as shown in Fig.4.

Then,

$$r=r_1+j\Delta r,\ j=0,\ 1,\ 2,...,N \tag{7}$$

$$L=r_2-r_1=N\Delta r \tag{8}$$

$$t=n\Delta t,\ n=0,\ 1,\ 2,\ 3... \tag{9}$$

The temperature T can be expressed as:

$$T(r,t)=T(j\Delta r,n\Delta t)\equiv T_j^n \tag{10}$$

Through finite difference method, Eq.(1) can be rewritten as:

$$\frac{T_{j-1}^n-2T_j^n+T_{j+1}^n}{(\Delta r)^2}+\frac{1}{r}\frac{T_{j+1}^n-T_{j-1}^n}{2\Delta r}=\frac{1}{a}\frac{T_j^{n+1}-T_j^n}{\Delta t} \tag{11}$$

Substituting Eq.(7)~(9) into Eq.(11) leads to:

$$T_j^{n+1}=(1-\frac{1}{2j})mT_{j-1}^n+(1-2m)T_j^n+(1+\frac{1}{2j})mT_{j+1}^n,\ j=1,\ 2,\ 3...,N-1;\ n=0,\ 1,\ 2... \tag{12}$$

Its magnitude of truncation error is $(\Delta r)^2+(\Delta t)$. m is Fourier number, expressed as:

$$m=\frac{a\Delta t}{(\Delta r)^2} \tag{13}$$

Through the boundary conditions $r=r_1$ and $r=r_2$ at the forward difference and backward difference, respectively, we can get:

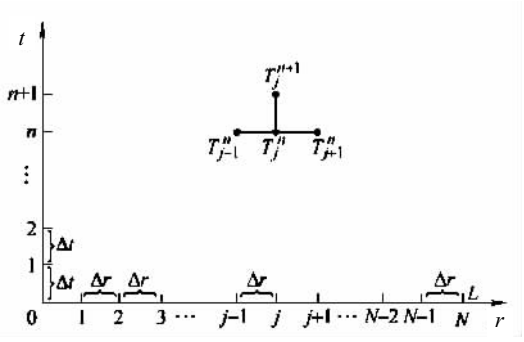

Fig.4 Discretization of area (r, t)

$$-\lambda\frac{T_1^{n+1}-T_0^{n+1}}{\Delta r}+h_1T_0^{n+1}=f_1 \tag{14}$$

$$\lambda\frac{T_N^{n+1}-T_{N-1}^{n+1}}{\Delta r}+h_2T_N^{n+1}=f_2 \tag{15}$$

Sorting Eq.(14) and (15), we can obtain their corresponding equivalent form as follows:

$$T_0^{n+1}=\frac{1}{1+(h_1\Delta r/\lambda)}[T_1^{n+1}+\frac{f_1\Delta r}{\lambda}],\ n=0,\ 1,\ 2,... \tag{16}$$

$$T_N^{n+1}=\frac{1}{1+(h_2\Delta r/\lambda)}[T_{N-1}^{n+1}+\frac{f_2\Delta r}{\lambda}],\ n=0,\ 1,\ 2,... \tag{17}$$

Its magnitude of truncation error is Δr. Eq.(2) can also be rewritten as:

$$T_j^0=T(j\Delta r)\equiv T(r),\ j=0,\ 1,\ 2,...,N \tag{18}$$

At this point, we obtain all the differential expressions of the heat conduction equations, as follows:

$$T_j^0=T(j\Delta r)\equiv T(r),\ j=0,\ 1,\ 2,...,N \tag{19-1}$$

$$T_0^{n+1}=\frac{1}{\beta_1}(T_1^{n+1}+\gamma_1),\ j=0 \tag{19-2}$$

$$T_1^{n+1}=(1-2m+\frac{m}{2\beta_1})T_1^n+\frac{3}{2}mT_2^n+\frac{m\gamma_1}{2\beta_1},\ j=1 \tag{19-3}$$

$$T_j^{n+1}=(1-\frac{1}{2j})mT_{j-1}^n+(1-2m)T_j^n+(1+\frac{1}{2j})mT_{j+1}^n,\ j=2,...,N-2 \tag{19-4}$$

$$T_{N-1}^{n+1}=\frac{2N-3}{2N-2}mT_{N-2}^n+(1-2m+\frac{m}{\beta_2}\frac{2N-1}{2N-2})T_{N-1}^n+\frac{m\gamma_2}{\beta_2}\frac{2N-1}{2N-2},\ j=N-1 \tag{19-5}$$

$$T_N^{n+1}=\frac{1}{\beta_2}(T_{N-1}^{n+1}+\gamma_2),\ j=N \tag{19-6}$$

Here,

$$n=0,\ 1,\ 2,...\text{and}\ \beta_i=1+\frac{h_i\Delta r}{\lambda},\ \gamma_i=\frac{f_i\Delta r}{\lambda}(i=1,2)$$

Eq.(19) is the explicit form of the difference equation. In order to ensure the convergence of the solution, the following condition must be satisfied:

$$m\equiv\frac{a\Delta t}{(\Delta r)^2}\le\frac{1}{2} \tag{20}$$

2.4 Calculation of convective heat transfer coefficient

2.4.1 Coefficient of inner wall of the roll

When the size of the hole and the type of fluid are determined, the heat transfer coefficient between the fluid and inner wall is related to the temperature and velocity of the fluid. The heat transfer coefficient is solved under different conditions at different temperatures of 125, 150, 175, 200 °C and different velocities of 0.31, 0.46, 0.61, 0.76 m/s. The temperature and velocities are randomly combined to generate 16 groups of heating conditions.

The roll is static and placed horizontally in the test. The heat transfer between the inner wall of the roll and thermal oil is forced convective heat transfer, of which the Nusselt number N_u is expressed as[15]:

$$N_u = C(R_e P_r)^n \tag{21}$$

where R_e is Reynolds number, P_r is Prandtl number, and C and n are constants determined by the flow pattern.

R_e is expressed as:

$$R_e = \frac{u_m d}{v} \tag{22}$$

P_r is expressed as:

$$P_r = \frac{c\rho v_i}{\lambda} \tag{23}$$

where u_m, v_i, ρ, λ, c are the velocity, kinematic viscosity, density, heat conduction coefficient, and specific heat of thermal oil, respectively. d is the diameter of the oil hole.

According to the basic principle of heat transfer, the flow of fluid in the pipe can be divided into three categories: laminar flow, transitional flow and turbulence flow according to R_e as follows [15]:

$$\begin{cases} R_e < 2300, \text{ laminar flow} \\ 2300 < R_e < 10\ 000, \text{transitional flow} \\ R_e > 2300, \text{ turbulence flow} \end{cases} \tag{24}$$

In case of $R_e > 2300$, N_u is expressed as [16]:

$$N_u = 0.027(1+(\frac{d}{l})^{0.7})R_e^{0.8}P_r^{1/3}(\frac{u_f}{u_w})^{0.25} \tag{25}$$

In case of $2300 < R_e < 10\ 000$, N_u is expressed as [16]:

$$N_u = 0.027(1+(\frac{d}{l})^{0.7})(1-\frac{6\times10^5}{R_e^{0.8}})R_e^{0.8}P_r^{1/3}(\frac{u_f}{u_w})^{0.25} \tag{26}$$

where u_f, u_w are the dynamic viscosity of the thermal oil when the temperatures of thermal oil and wall are the qualitative temperature. l is the length of oil hole.

The convective heat transfer of the inner wall of the roll can be calculated:

$$h_1 = \frac{N_u \lambda}{d} \tag{27}$$

2.4.2 Coefficient of outer wall of roll

The heat transfer between the outer wall of the roll and air is natural convection, of which the Nusselt number N_u is expressed as[16]:

$$N_u = C(G_r P_r)^n \tag{28}$$

where P_r is Prandtl number, C and n are constants determined by roll placement and the flow pattern, respectively. The related parameters are listed in Table 1.

The Grashof number G_r is expressed as:

$$G_r = \frac{g\alpha L^3(t_w - t_a)}{v^2} \tag{29}$$

where g is the gravitational acceleration, t_w is the temperature of outer wall of roll, and t_a is the temperature of ambient air, which is equal to 20 °C; L is characteristic dimension of roll and α is cubical expansion coefficient of air. The performance parameters of air at 20 °C are shown in Table 2.

The convective heat transfer of the outer wall of the roll can be calculated from:

$$h_2 = \frac{N_u \lambda}{L} \tag{30}$$

3 Simulation of Temperature Field of the Roll

3.1 Model establishment

Depending on the size of the roll and thermal oil shown in Fig.5 and 6, three-dimensional model was built, as shown in Fig.7. Related material parameters of the roll and thermal oil are listed in Tables 3 and 4.

Table 1 Parameters of Eq.(28)

Way of roll placement	Flow pattern	C	n	G_rP_r	Characteristic dimension selection
Horizontal cylinder	Laminar flow	0.53	1/4	10^4~10^9	Outer diameter
Horizontal cylinder	Turbulence flow	0.13	1/3	10^9~10^{12}	Outer diameter

Table 2 Performance parameters of air

Density /kg·m^{-3}	Specific heat/ J·(kg·°C)$^{-1}$	Thermal conductivity/ W·(m·°C)$^{-1}$	Kinematic viscosity/ ×10^{-6} m^2·s^{-1}	P_r	Cubical expansion coefficient/K
1.205	1005	0.0259	15.06	0.703	3.411×10^{-3}

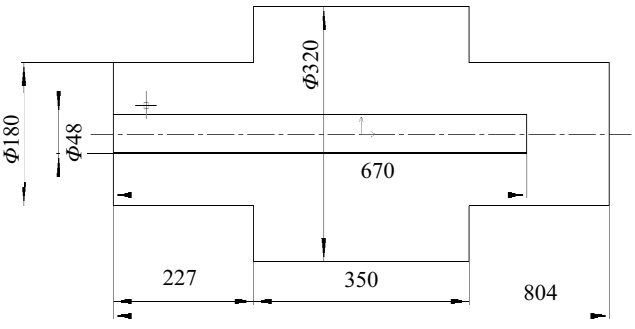

Fig.5 Dimension drawing of the roll (mm)

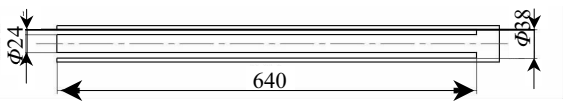

Fig.6 Dimension drawing of thermal oil (mm)

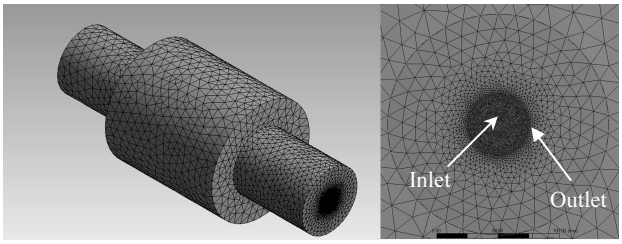

Fig.7 Diagram of three-dimensional model

Under the conditions of different temperatures of 125, 150, 175 and 200 °C and different velocities of 0.31, 0.46, 0.61 and 0.76 m/s, the temperature and velocities are randomly combined to generate 16 groups of simulations. The initial temperature of the roll is 20 °C.

The simulation requires the setting of the temperature and velocity of thermal oil. In addition, the convection heat transfer coefficient should be settled, and the specific parameters should be selected according to Tables 5 and 6.

3.2 Simulation results

The simulation of temperature field was carried out by the nonlinear finite element software FLUENT.

Fig.8 shows that at different flow velocities, the roll surface temperature rises from 20 °C to 81, 87, 93 and 96 °C within 130 min (T_0=125 °C). Fig.9 shows that at different flow velocities, the roll surface temperature rises from 20 °C to 130, 140, 146 and 152 °C within 140 min (T_0=200 °C). Fig.10 shows the roll cross-section temperature distribution at different flow rates (T_0=125 °C). Fig.11 shows roll cross-section temperature distribution at different flow rates (T_0=200 °C).

Fig.8~11 show the nephogram of the surface and cross-section temperature distribution of the roll under different heating conditions. It can be concluded that:

1) The roll temperature distribution is uniform in the circumferential direction because of the structural design of the roller.

2) In the axial direction, the temperature near the roll operating side is the highest and the temperature decreases gradually from the operating side to the driving side. The temperature difference between the operating side and the driving side is very small and is almost unaffected by the fluid temperature and speed.

3) In the radial direction, the temperature of the center is the highest and drops gradually from inside to outside. The temperature difference between the inner wall and the outer wall of the roller is very small, and is almost not affected by the temperature and speed of the fluid.

4) At the same fluid temperature, the roll temperature increases with increasing the flow velocity. At the same flow velocity, the roll temperature increases with increasing the temperature of thermal oil.

Table 3 Material parameters of the roll

Material	Density/ kg·m^{-3}	Specific heat/ J·(kg·°C)$^{-1}$	Thermal conductivity/ W·(m·°C)$^{-1}$
9Cr2Mo	7800	860	49.8

Table 4 Performance parameters of L-QD330 at different temperatures

Temperature/ °C	Density/ kg·m^{-3}	Specific heat/ J·(kg·°C)$^{-1}$	Thermal conductivity/ W·(m·°C)$^{-1}$	Kinematic viscosity/ ×10^{-6} m^2·s^{-1}
20	863.7	1777	0.139	71.2
125	811.9	2179	0.130	2.50
150	799.5	2275	0.128	1.83
175	787.2	2371	0.126	1.58
200	774.8	2467	0.124	1.49

3.3 Experimental results

Fig.12 shows the temperature rise curve of the roll surface average temperature under different heating conditions. Fig.12a shows that when the thermal oil is heated for 110 min, the roll surface temperature rises at a very slow rate and the temperature increases at a rate of 1 °C/5 min on average. Therefore, heating is stopped after 125 min. Fig.12b shows that when the thermal oil is heated for 120 min, the temperature of the roll rises at a very slow rate and the temperature increases at a rate of 1 °C/5 min on average. Therefore, heating is stopped after 140 min. Fig.12c shows that when the thermal oil is heated for 120 min, the temperature of the roll rises at a very slow rate and the temperature rises at a rate of 1 °C/8 min on average. Therefore, heating is stopped after 140 min. Fig.12d shows that when the thermal oil is heated for 120 min, the temperature of the roll rises at a very slow rate and the temperature is increased at a rate of 1 °C/5 min on average. Therefore, heating is stopped after 140 min.

Fig.12 indicates that when the heating is stopped, the roll surface temperature continues to increase due to the temperature difference between the inner wall and the outer side of the roll, and then gradually decreases under the influence of natural convection. The extended time has a little relation with the fluid temperatures and velocities, which is about 5~8 min. Fig.12 also indicates that under different fluid temperatures

Table 5 Criterion number and convective heat transfer coefficient of inner wall of the roll

Heating condition (temperature/°C-velocity/m·s^{-1})	R_e	P_r	Flow pattern	N_u	h_1/W·(m·°C)$^{-1}$
125-0.31	5952	34.02	Transitional	35.34	95.70
125-0.46	8832	34.02	Transitional	51.08	138.3
125-0.61	11712	34.02	Turbulent	67.20	182.0
125-0.76	14592	34.02	Turbulent	80.12	217.0
150-0.31	8131	26	Transitional	39.96	106.6
150-0.46	12065	26	Turbulent	57.98	154.6
150-0.61	16000	26	Turbulent	72.66	193.7
150-0.76	19934	26	Turbulent	86.64	231.0
175-0.31	9417	23.4	Transitional	42.23	110.8
175-0.46	13974	23.4	Turbulent	60.45	158.7
175-0.61	18531	23.4	Turbulent	75.77	198.9
175-0.76	23088	23.4	Turbulent	90.34	237.1
200-0.31	9986	22.97	Transitional	43.36	112.0
200-0.46	14818	22.97	Turbulent	61.80	159.6
200-0.61	19651	22.97	Turbulent	77.45	200.1
200-0.76	24483	22.97	Turbulent	92.35	238.6

Table 6 Criterion number and convective heat transfer coefficient of outer wall of the roll

Characteristic dimension/m	G_r	$G_r P_r$	Flow pattern	N_u	h_2/W·(m·°C)$^{-1}$
0.32	1.93×10^8	1.36×10^8	Laminar	57.21	4.63
0.18 (operation)	5.16×10^7	3.63×10^7	Laminar	41.13	5.92
0.18 (driving)	3.44×10^7	2.42×10^7	Laminar	37.16	5.34

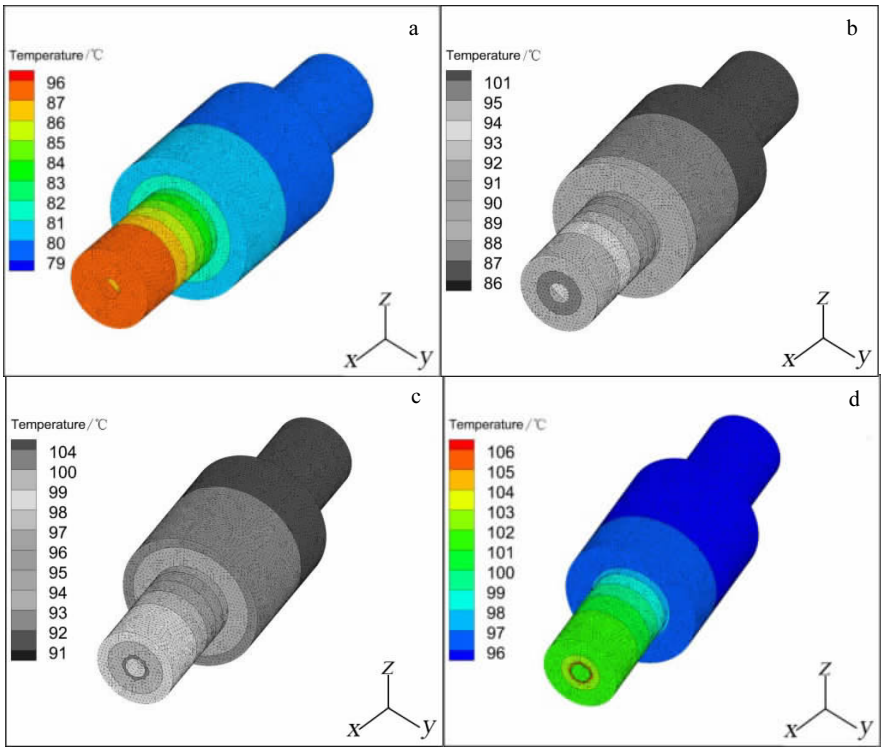

Fig.8 Nephogram of roll surface average temperature under different fluid velocities at thermal oil temperature of 125 °C: (a) v=0.31 m/s, (b) v=0.46 m/s, (c) v=0.61 m/s, and (d) v=0.76 m/s

and velocities, the temperature of the roll rises with decreasing the rate, and when the fluid temperature rises and the velocity increases, the temperature of the roll rises faster.

Fig.13 shows that the roll surface temperature distribution has the characteristics of high temperature on the operating side and low temperature on the driving side. The temperature difference between the two sides is 5~12 °C. The average temperature of the roll surface is approximately the same as that of the cross section of the roll because of the characteristic.

3.4 Comparison between theoretical and experimental values

Fig.14 is a comparison between the simulated and experi-

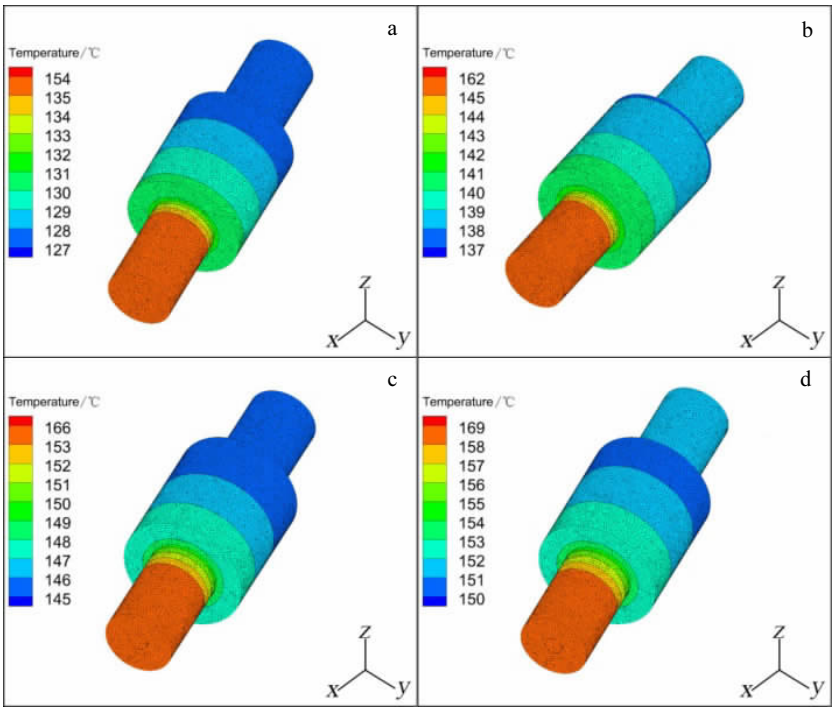

Fig.9 Nephogram of roll surface average temperature under different fluid velocities at thermal oil temperature of 200 °C: (a) v=0.31 m/s, (b) v=0.46 m/s, (c) v=0.61 m/s, and (d) v=0.76 m/s

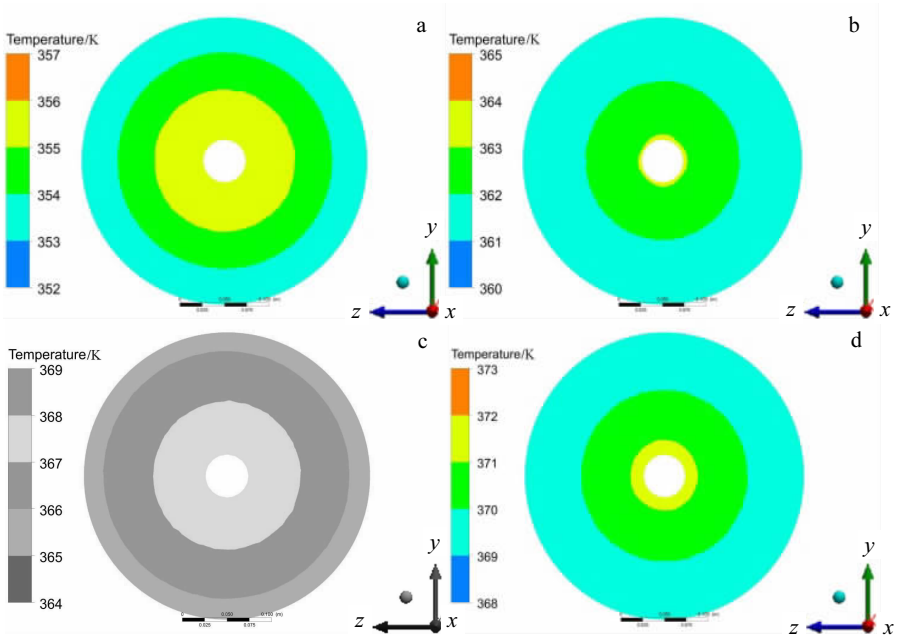

Fig.10 Nephogram of cross-section temperature distribution of the roll under different fluid velocities at thermal oil temperature of 125 °C: (a) v=0.31 m/s, (b) v=0.46 m/s, (c) v=0.61 m/s, and (d) v=0.76 m/s

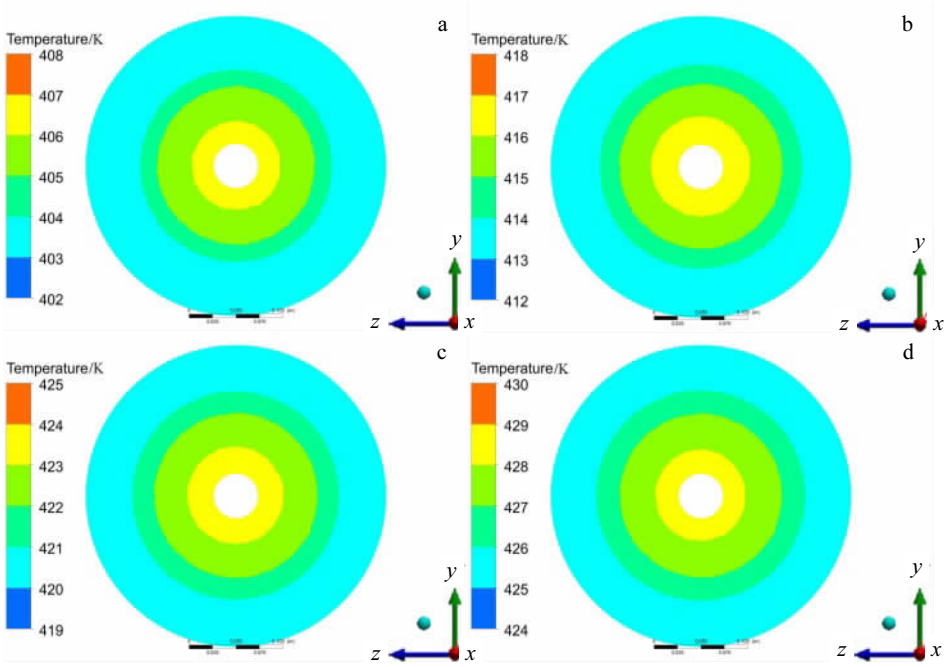

Fig.11 Nephogram of roll cross-section temperature distribution under different fluid velocities at thermal oil temperature of 200 °C: (a) v=0.31 m/s, (b) v=0.46 m/s, (c) v=0.61 m/s, and (d) v=0.76 m/s

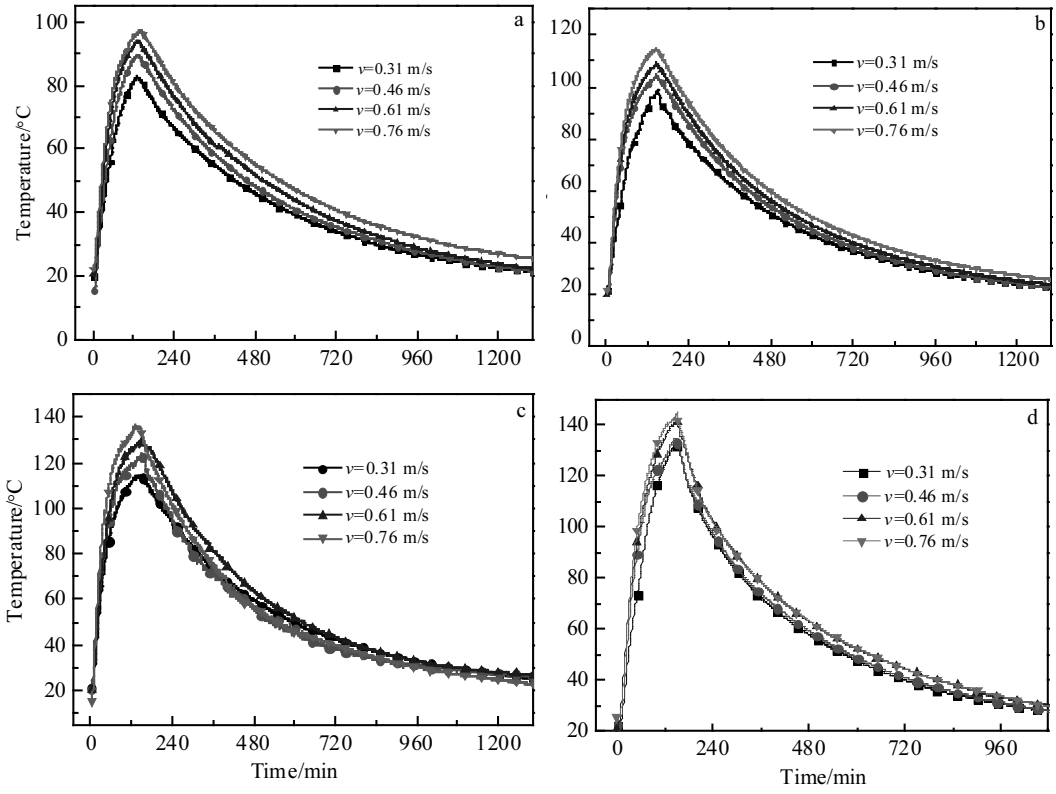

Fig.12 Temperature rise curves of the roll surface average temperature under various fluid temperatures and velocities: (a) T_0=125 °C, (b) T_0=150 °C, (c) T_0=175 °C, and (d) T_0=200 °C

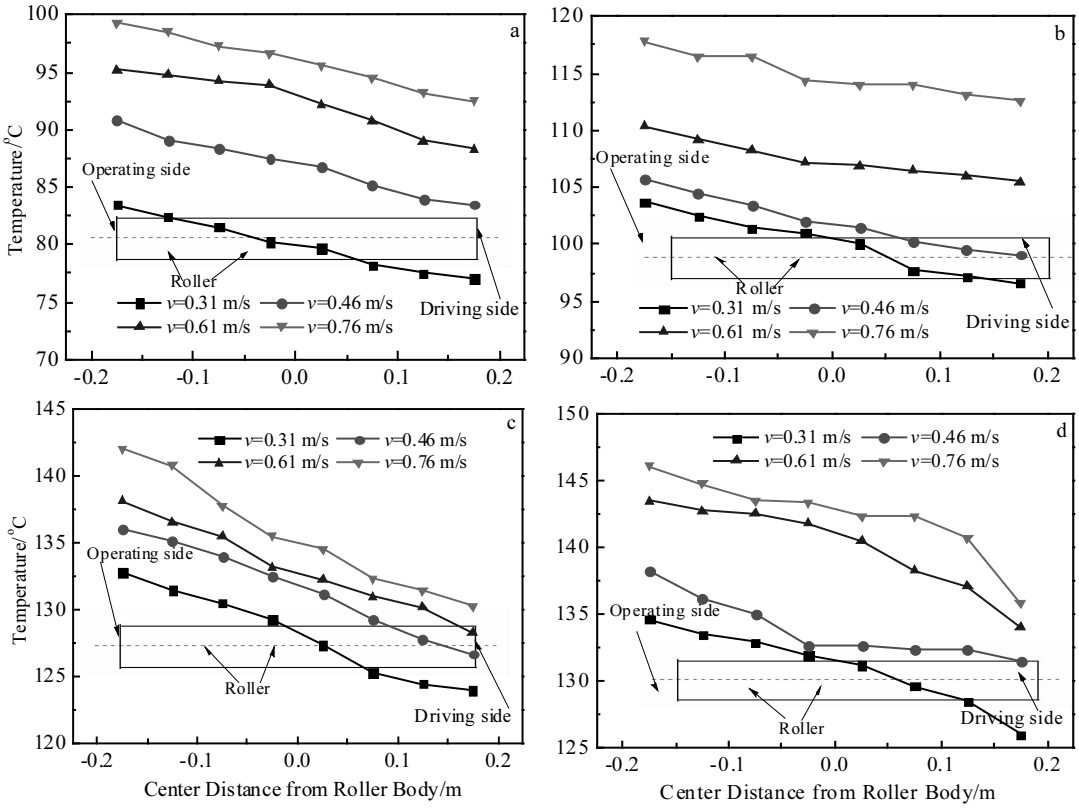

Fig.13 Roll temperature distribution when heating is stopped: (a) T_0=125 °C, (b) T_0=150 °C, (c) T_0=175 °C, and (d) T_0=200 °C

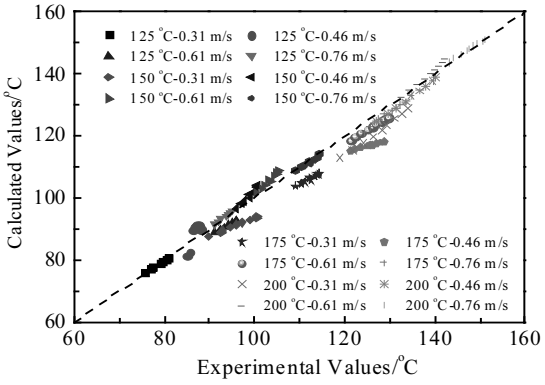

Fig.14 Comparison between the calculated and experimental values after heating for 100 min

mental values, and the heating time is 100~140 min. The maximum relative error between them is shown in Table 7.

The sources of error are mainly as follows: the physical parameters of roll and thermal oil vary with temperature; the convection heat transfer coefficient varies with temperature. The relative error δ can be expressed as follows:

$$\delta = \left| \frac{T_s - T_e}{T_e} \right| \times 100\% \quad (31)$$

Table 7 Contrast between calculated values T_c and experimental values T_e of average temperature T

Heating condition (temperature/°C –velocity/m·s^{-1})	Maximum relative error/%
125-0.31	7.96
125-0.46	4.79
125-0.61	3.59
125-0.76	0.99
150-0.31	2.29
150-0.46	3.38
150-0.61	3.64
150-0.76	0.99
175-0.31	5.88
175-0.46	8.30
175-0.61	2.88
175-0.76	2.49
200-0.31	3.73
200-0.46	2.14
200-0.61	2.01
200-0.76	0.18

As shown in Table 7: (1) the simulation and experimental values of the temperature rise agree well and the maximum relative error is 8.3%; (2) fluid-solid coupled heat transfer of roll can be solved by simulation analysis, which provides an effective and practical method for calculating the roll temperature field.

4 Conclusions

1) In the axial direction under different heating conditions, the temperature near the roll operating side is the highest and decreases gradually from the operating side to the driving side. The temperature difference range between the operating side and the driving side is 5~12 °C, which is almost unaffected by the fluid temperature and speed.

2) In the radial direction under different heating conditions, the temperature of the center is the highest and drops gradually from inside to outside. The maximum temperature difference between the inner wall and the outer wall of the roller is 6 °C, which is almost unaffected by the temperature and speed of the fluid. The roll temperature is distributed uniformly in the circumferential direction because of the structural design of the roller.

3) At different fluid temperatures and velocities, the temperature of the roll rises with decreasing the rate, and when the fluid temperature rises and the velocity increases, the temperature of the roll rises faster.

4) After the heating for the roll is stopped, its surface temperature does not immediately begin to drop and remains for a period of time, about 5~8 min. The temperature and speed of the fluid have less effect on the extended time.

5) The calculated values of the average roll surface temperature agree well with the experimental values, and the maximum relative error is 8.3%. The overall results are consistent, which verifies the correctness and effectiveness of the finite difference model.

References

1 Mordike B L, Ebert T. *Materials Science and Engineering A*[J], 2001, 302(1): 37

2 Jia W T, Le Q Z. *Materials and Design*[J], 2017, 121: 288

3 Tang Y, Jia W T, Liu X *et al*. *Materials Science and Engineering A*[J], 2017, 689: 332

4 Liu J L, Yu H J, Chen C Z *et al*. *Optics and Lasers in Engineering*[J], 2017, 93: 195

5 Jia W T, Tang Y, Le Q C *et al*. *Journal of Alloys and Compounds*[J], 2017, 695: 1838

6 Beausir B, Biswas S, Kim D L *et al*. *Acta Materialia*[J], 2009, 57(17): 5061

7 Wang Lingyun, Huang Guangjie, Chen Lin *et al*. *Rare Metal Materials and Engineering*[J], 2007, 36(5): 910 (in Chinese)

8 Zhang Tingting, Zhang Chunwei. *Baosteel Technology*[J], 2016, 5: 55 (in Chinese)

9 Li Tingting, Zhou Yueming, Shu Da. *Heat Treatment of Metals*[J], 2016, 8: 166 (in Chinese)

10 Bergara A, Dorado J I, Martin-Meizoso A *et al*. *International Journal of Fatigue*[J], 2017, 103: 112

11 Yan Y Z, Shi M J, Wang Q *et al*. *Journal of Crystal Growth*[J], 2017, 468: 923

12 Shi Y, Yao Y P. *International Journal of Heat and Mass Transfer*[J], 2017, 107: 339

13 Cai J, Huai X L. *Applied Thermal Engineering*[J], 2010, 30: 715

14 Yu Changming. *Heat Conduction*[M]. Beijing: Higher Education Press,1983: 506 (in Chinese)

15 Yang Shiming, Tao Wenquan. *Heat Transfer*[M]. Beijing: Higher Education Press, 2006: 197 (in Chinese)

16 Wang Houhua. *Heat Transfer*[M]. Chongqing: Chongqing University Press, 2006: 156 (in Chinese)

镁合金温控轧辊的温度场

李 洋[1]，马立峰[1]，姜正义[2]，黄志权[1]，林金宝[1]，姬亚峰[1]

(1. 太原科技大学 重型机械教育部工程研究中心，山西 太原 030024)

(2. 伍伦贡大学，伍伦贡 NSW 2522, 澳大利亚)

摘 要：采用导热油循环流动传热的方式对轧辊进行温度控制，基于有限差分法建立了轧辊、导热油传热过程的差分模型，利用FLUENT 建立了导热油加热轧辊的流固耦合传热模型，并辅以相应的实验验证，给出了其传热过程中轧辊的温升曲线、辊身表面及横截面温度分布。结果表明：在不同的加热条件下，其表面温度分布呈现操作侧温度高、驱动侧温度低的特点，两端的温差范围在5~12 ℃，且流体温度与速度对其影响较小；轧辊内壁与外壁的最大温差 6 ℃，可近似认为径向温度分布均匀；随着加热时间的增加，轧辊表面温度均呈速率减小的趋势上升，流体温度升高及速度增大时，轧辊温升变快；轧辊停止加热后，其表面温度不会立即下降且持续增长一段时间，约为 5~8 min，流体的温度和速度对延长的时间影响较小；轧辊表面平均温度的计算值与实验值吻合较好，最大相对误差为 8.3%，表明该模型可正确预测轧辊表面的平均温度，作为镁合金板材轧制模型的一部分，利于轧制过程中轧辊的等温控制，实现镁合金板材的等温轧制控制。

关键词：镁合金；有限差分法；耦合传热模型；温升曲线；温度分布；等温轧制

作者简介：李 洋，男，1993 年生，硕士，太原科技大学重型机械教育部工程研究中心，山西 太原 030024，电话：0351-2776769，E-mail: liyang930914@163.com